Effect of the crystal chemistry on the hydration mechanism of swelling micas

Esperanza Pavón[*1], *María D. Alba*[1], *Miguel A. Castro*[1], *A. Cota*[2], *Francisco J. Osuna*[1] *and M. Carolina Pazos*[3]

[1] Instituto Ciencia de los Materiales de Sevilla- Departamento de Química Inorgánica, CSIC-Universidad de Sevilla. Avda. Américo Vespucio, 49. 41092, Sevilla. Spain

[2] Laboratorio de Rayos X. CITIUS. Universidad de Sevilla. Av. Reina Mercedes s/n, Sevilla, Spain

[3] Escuela de Ciencias Químicas, Universidad Pedagógica y Tecnológica de Colombia UPTC. Avda. Central del Norte, Vía Paipa, Tunja, Boyacá, Colombia

Abstract

Swelling and dehydration under minor changes in temperature and water vapor pressure is an important property that clays and clay minerals exhibit. In particular, their interlayer space, the solid-water interface and the layers' collapse and re-expansion have received much attention because it affects to the dynamical properties of interlayer cations and thus the transfer and fate of water and pollutants. In this contribution, the dehydration and rehydration mechanism of a swelling

[*] *E-mail address*: esperana.pavon@gmail.com

high-charge mica family is examined by in situ X-ray Diffraction. The effect of the aluminosilicate layer charge and the physicochemical properties of the interlayer cations on these processes are analyzed. The results showed that the dehydration temperature and the number of steps involved in this process are related to the layer charge of the silicate and the physicochemical properties of the interlayer cations. Moreover, the ability to adsorb water molecules in a confined space with high electric field by the interlayer cations does not only depend on their hydration enthalpy but also on the electrostatic parameters of these cations.

KEYWORDS: Water adsorption; clays; swelling interlayer; 2:1 layer phyllosilicates; hydration; dehydration

1. INTRODUCTION

Clays and clays minerals are largely used in several engineering applications because of their ability to adsorb and immobilize hazardous species (Vieillard et al., 2011). They can be used as pollution control, carriers of pesticides, construction materials or catalysts as well as to serve as active principle carriers or excipients, converting these materials beneficial to human health (Amato, 2013; Bergaya et al., 2006; Carretero, 2002; Carretero and Pozo, 2009; Hanczyc et al., 2003; Macewan, 1948). Recently, clays and clay minerals are being used as liners in waste disposal and barriers in nuclear waste management. In fact, they are a key factor on the engineered barrier system (EBS) of deep geological repositories (DGRs) (Osuna et al., 2015).

The sensitivity to minor changes in temperature and water vapor pressure is an important property of clays in a geologic repository. Among clays and clay minerals, 2:1 swelling phyllosilicates (smectites and vermiculites) have been extensively analyzed due to their hydration and rehydration properties that made them so useful in the above applications (Ferrage et al., 2005; Salles et al., 2010; Salles et al., 2007; Salles et al., 2008; Salles et al., 2013) . In particular, their interlayer space, the solid-water interface and the layers collapse and re-expansion have received attention because they affect the dynamical properties of interlayer cations and thus the transfer and fate of water and pollutants (Malikova et al., 2007; Malikova et al., 2010; Marry et al., 2011; Michot et al., 2005; Michot et al., 2012; Rinnert et al., 2005). The changes associated with the water content on the interlayer space of clay minerals have also significant impact on CO_2 storage capacity (Schaef et al., 2015). In addition, the presence of phyllosilicates on the Martian surface increased the interest of clay mineral−water reactions (Meunier et al., 2012).

During many decades, the ability of the 2:1 phyllosilicates to incorporate water molecules in the interlayer space and the corresponding change in the basal space of these materials have been studied (Suter et al., 2015). For example, Bradley (Bradley et al., 1937) showed, using X-ray Diffraction (XRD) that the basal spacing of smectites increases in discrete steps as a function of increasing water amount. These transitions were later attributed to the intercalation of 0, 1, 2 or 3 water layers (0W, 1W, 2W or 3W) in the interlayer space of the smectites (Mooney et al., 1952a, b; Norrish, 1954). More recently, Dazas et al. (Dazas et al., 2015) studied the impact of smectite crystal chemistry on its hydration using XRD profile modeling and Monte Carlo simulations. For a given hydration state, hydroxylates saponites showed a constant water content and no influence of the layer charge was found. Molecular dynamics and grand canonical Monte Carlo simulations were used to study the effects of layer charge location, interlayer cation, and temperature on the swelling of montmorillonite and beidellite (Teich-McGoldrick et al., 2015; Zabat and Van Damme, 2000).

Hence, the hydration properties of 2:1 phyllosilicates appears governed by the origin of the layer charge (tetrahedral/octahedral) and the quantity and nature of the interlayer cation. Consequently, the swelling behavior depends on the repulsive forces relating to the interactions between the 2:1 layers and the attractive forces between the interlayer cation and the negative charged siloxane surface (Laird, 1999; Norrish, 1954; Pavón et al., 2014).

There is a considerable interest in a series of synthetic sodium fluorophlogopites, known as Na-n-mica, which exhibit a high permanent negative charge caused by aluminium substitution in the tetrahedral sheet of the crystal lattice (Park et al., 2002). The greater the degree of substitution, the more dense the negative charge, ranging it from 2 to 4 when the Si/Al ratio is equal to 6/2 and 1/1 respectively. Unlike phlogopite, these materials have significant swelling

capabilities and applications as decontaminants and storage media (Alba et al., 2006; Gregorkiewitz and Rausell-Colom, 1987; Park et al., 2002). These swelling high-charged micas, in which the layer charge can be adjusted, may be valuable for the decontamination of harmful heavy metal cations (Ravella et al., 2008) via ion-exchange reactions and for the selective removal of radioactive ions (Alba et al., 2006) and hydrocarbon molecules (Alba et al., 2011) (Pazos et al., 2017). Recently, it has been observed that the formation of Inner Sphere Complexes (ISC) by the cations in the interlayer space of swelling high charge mica was favored when the aluminum content in the tetrahedral layer increased (Pavón et al., 2014). Consequently, the reversibility of the collapse and re-expansion of the layers will be influenced by the ratio ISC/OSC (Outer Sphere Complexes), controlling the adsorption of pollutants or the release of nutrients or drugs.

Hence, this contribution describes the hydration behavior of these materials and: 1) analyze the influence of temperature on the dehydration process, 2) evaluate the rehydration as a function of relative humidity, and, 3) establish the parameters that govern the collapse and re-expansion of these high charged swelling micas. Synthetic micas with different total layer charge (n=2, 3 and 4) and five different interlayer cations were selected (Na^{+}, Li^{+}, K^{+}, Mg^{+2} and Al^{+3}). In situ and at real time XRD analysis at variable temperature and humidity were performed.

2. MATERIALS AND METHODS

2.1.Samples.

A procedure similar to that of Alba et al.(Alba et al., 2006) was employed. Stoichiometric powder mixtures with the molar compositions (8 − n) SiO_2, (n/2) Al_2O_3, 6 MgF_2, and (2n) NaCl were used to synthesize Na-n-Mica (n = 2, 3, 4). The starting materials were SiO_2 from Sigma (CAS No. 112945-52-5, 99.8% purity), $Al(OH)_3$ from Riedel-de Haën (CAS no. 21645−51−2,

99% purity), MgF_2 from Aldrich (CAS No. 20831-0, 98% purity), and NaCl from Panreac (CAS No. 131659, 99.5% purity). All reagents were mixed and vigorously ground before heating to 900 °C in a Pt crucible for 15 h. After cooling, the solids were washed with deionized water and dried at room temperature. The as-synthesized samples, Na-n-Mica (n ranging between 2 and 4) were analyzed by X-ray diffraction (XRD) to evaluate their purity. Their structural formulae is $Na_n[Si_{8-n}Al_n]Mg_6O_{20}F_4$ where n ($2 \leq n \leq 4$) is the layer charge**.**

2.2.Cation-Exchange Process.

Na-n-Mica were exchanged with solutions of Li^+, K^+, Mg^{2+}, and Al^{3+} salts at concentrations that ensured that the molar content of the cation was 10 times the cation-exchange capacity (CEC) of the mica (Pavón et al., 2013). The most important characteristics of these ions in solution are displayed in Table 1S (Supporting Information). The reagents used were $MgCl_2$ from Sigma-Aldrich (CAS No. 7786-30-6, 99.99% purity), KCl from Fluka (CAS No. 7447-40-7, >99% purity), $AlCl_3$ from Fluka (CAS No. 7784-13-6, >99.0% purity), and LiCl from Fluka (CAS No. 7447-41-8, >99.0% purity). The ion-exchange process was described elsewhere (Pavón et al., 2013) and the purity of the samples analyzed by XRD (Pavón et al., 2014). This exchange method prevents the modification of the silicate framework and consequently, XRF analyses were not needed. The extent of the cation exchange reaction was monitored by ^{23}Na MAS NMR (not shown). These solids are referred as X-n-Mica, where X = Na^+, Li^+, K^+, Mg^{2+}, or Al^{3+} and n = 2, 3, or 4.

2.3.Sample Characterization. X-ray diffraction patterns at variable temperature (VT-XRD) and humidity (VH-XRD) were obtained at the CITIUS X-ray laboratory (University of Seville, Spain) using a reaction chamber, Anton Paar TTK450, connected to a Bruker D8 Advance instrument equipped with a Cu Kα radiation source and θ/θ configuration. The powder XRD

patterns were obtained in the 2θ-range 3−12° with a step size of 0.03° and a time step of 25 s. Variable humidity experiments were performed by adding a Sycos Humidity Controller to the diffractometer. The analysis of the peaks was performed by pseudo-Voight functions fitting using TOPAS© software from Bruker.

Temperature experiments consisted of four stages (Fig. 1 a):

1. Initial stage: samples where heated at 30 ºC for 3h to ensure the stability of the hydration state at near room temperature.
2. Dehydration stage: samples were heated from 30 ºC to 300 ºC with a heating rate of 1 $°C \cdot min^{-1}$.
3. Cooling stage: samples were unrestricted cooled to 30 ºC. When this temperature was reached, XRD difractograms were obtained during 3h to determine if the samples could be free rehydrated.
4. Forced rehydration: a water drop was added to the sample to examine the swelling capacity of the dehydrated micas.

Humidity experiments consisted of four stages (Fig. 1b):

1. Initial stage: At room temperature and humidity
2. Sample dehydration: temperature was increased to 100 ºC with a heating rate of 10 $°C \cdot min^{-1}$ and maintained for one hour, having a constant dry N_2 flux in the chamber.
3. Cooling stage: samples were cooled to room temperature with a constant dry N_2 flux in the chamber to avoid spontaneous hydration.
4. Variable humidity: humidity was increased in discrete steps, varying from 0% to nearly 90% relative humidity (RH). At each step and after the humidity stabilized, XRD difractograms were recorded.

3. RESULTS

Fig. 2 and 3 represent the basal spacing (d_{001}) for the two set of experiments described above, temperature (Fig. 2) and humidity (Fig. 3).

In the temperature experiment, Stage 1 was performed to stabilize the hydration state at room temperature. Basal spacings remained constant for each sample (Fig. 2, stage 1, Table 1), indicating that their hydration states are constant with time. The values are 12 to 14 Å and correspond to the previously observed values in these materials (Pavón et al., 2013). Bihydrated layers (2W) with H_2O on each side of the interlayer midplane produces a 001 reflection at d_{001}=14.9-15.7 Å (Ferrage et al., 2005). For monohydrated layers (1W), cations and H_2O are located in the interlayer midplane and the d_{001} values range between 11.6 and 12.9 Å (Ferrage et al., 2005). Dehydrated layers (0W), interlayer cation without water in the midplane, gives a d_{001}=9.7-10.2 Å (Ferrage et al., 2005). The layer-to-layer distances are shortened for fluorinated clay minerals (Dazas et al., 2015), and therefore, the observed values of ca. 12 Å and ca. 14 Å for F-rich samples are assigned to a 1W and 2W layers, respectively.

3.1. Dehydration processes.

The dehydration process was analyzed by changes in d_{001} values with increasing temperature; see stage 2 of the temperature experiment (Fig. 2, stage 2). As temperature increased, the basal spacing evolved, regardless of the initial interlayer cation or layer charge, to final values matching a collapsed interlayer space (d_{001}≈10Å, 0W, Table 1).

A single and abrupt transition was observed regardless the layer charge of the aluminosilicate in Na^+ and K^+ samples. The initial basal spacing (Table 1) characteristic of one monolayer of H_2O,

evolved to a collapsed interlayer at ca. 70 ºC in the Na-n-Mica and ca. 50 ºC in the K-n-Mica samples.

The change in the d_{001} value for Li-4-Mica is similar to the Na^+ and K^+ samples, a single transition from 12.05 Å (1W) to 10.2 Å (0W) at 79ºC was observed (Table 1). For Li-3-Mica, two initial reflections were observed at 14.4 Å (2W) and 12.1 Å (1W). The 14.4 Å peak disappeared at 37 ºC whereas the 12.1 Å peak suffered an abrupt transition at 79 ºC and evolved to a d_{001} value of 10.3 Å (0W). Li-2-Mica showed two d_{001} peaks at 14.5 Å (2W) and 12.1 Å (1W). The 14.5 Å peak disappeared at 169 ºC after two transitions at 41 ºC and 79 ºC where d_{001} values of 13.4 and 11.5 Å were found. The 12.1 Å peak suffered three transitions at 71-81 ºC (11.05 Å), 127 ºC (10.5 Å) and 195 ºC until it reached 10.1 Å.

Mg-n-Mica showed a more complex behavior depending on the layer charge of the silicate. Mg-4-Mica showed two reflections at room temperature (13.6 Å and 12.1 Å, 2W and 1W, respectively, Table 1). The 13.6 Å peak disappeared at 58 ºC, whereas the 12.1 Å peak produced a single transition at 120 ºC to 10.2 Å (0W). As the layer charge decreases, an increase in the number of steps in the dehydration process occurs (Fig. 2, stage 2). To reach the anhydrous state, the initial reflections that the Mg-3-Mica samples showed at room temperature, 14.4 Å (2W), 13.9 Å, (2W-1W) and 12.1 Å (1W) suffered different transitions at diverse temperatures. Moreover, Mg-2-Mica which showed only a reflection at room temperature (14.4 Å, 2W) evolved in three steps until reaching a basal spacing compatible with a collapse phase (10.05 Å, 0W).

Al-n-Mica produced a single but continuous transition where the initial basal spacing (2W) evolved to a collapsed basal spacing (0W).

3.2. Rehydration processes.

Uncontrolled rehydration was analyzed in the temperature experiment (Fig. 1a) during the 3rd and 4th stages.

For X-4-Mica, the free rehydration is only partial for the samples homoionized with sodium and lithium; samples with K^+, Mg^{+2} and Al^{+3} remained at the collapsed basal spacing that occurred after heating. When layer charge decreased, the rehydration is progressively reached for nearly each sample with K-n-Mica being an exception. These samples are not able to rehydrate naturally regardless the layer charge of the aluminosilicate, as ~~it has been~~ previously observed in others clays (Ferrage et al., 2005)

Stage 4 in the temperature experiment (Fig. 1 and 2, stage 4, Table 1) was performed to force the maximum hydration state of the samples. The observed behavior was similar that in stage 3. Samples with Li^+ and Na^+ reached their initial hydration state, independently of the silicate layer charge. However, K-n-Micas is only able to rehydrate when the layer charge is 2. Rehydration is obtained for n=3 for Mg^{+2} and for n=2 for Al^{+3}.

An analysis of the rehydration capacity with variable humidity is given in Fig. 3 where basal spacing is represented versus the humidity in the XRD chamber.

Li-4-Mica, Na-4-Mica and Mg-4-Mica are able to rehydrate from 0W, (ca. 10 A) to 1W (ca. 12 A). The humidity value where this transition occurs was different for each interlayer cation, being between 20 and 30%. However, K-4-Mica and Al-4-Mica samples were not able to rehydrate even for humidity near 100% RH. X-3-Mica and X-2-Mica samples were able to rehydrate, being the required humidity to produce the transition characteristic of each sample.

4. DISCUSSION

4.1. Dehydration processes.

As temperature increased, the basal spacing evolved, regardless of the initial interlayer cation or layer charge, to final values matching a collapsed interlayer space (d_{001}≈10Å, 0W, Table 1). However, the temperature where dehydration occurred and the number of steps involved in dehydration were determined by the layer charge of the silicate layer and the nature of the interlayer cation.

4.1.1. Layer charge influence.

Dehydration is affected by aluminosilicate layer charge. For the highest layer charge aluminosilicate, X-4-Mica, a single transition for each initial basal spacing regardless of the interlayer cation. For strong layer interactions, interlayer cation form inner sphere complexes (Pavon et al. 2014) and dehydration is a single step process. This mechanism will favor the immobilization of harmful cations. The decrease in the layer charge caused an increase of the number of dehydration steps and the temperature at which they occurred (Fig. 2). As layer charge decreases and interlayer cations form outer sphere complexes (Li-n-Mica, Mg-n-Mica and Al-n-Mica) (Pavón et al., 2014) the release of H_2O begin with the weaker bonded molecules and continue with the stronger bonded that require higher temperatures to be ejected from the interlayer.

4.1.2. Effect of physicochemical properties of interlayer cations

To analyze the influence of cationic radii on the dehydration mechanism attention must be focused on Li-n-Mica, Na-n-Mica and K-n-Mica, where the interlayer cation has the same charge but different cation radii (Table 1s S.I.).

Na^+ and K^+ samples exhibit the expected behavior for one monolayer of H_2O in the interlayer (Salles et al., 2008)(Fig. 2, stage 2). The higher temperature required for Na-n-Mica to initiate dehydration compared to K-n-Mica is the consequence of its smaller ionic radius and more negative hydration enthalpy that Na^+ exhibits. This abrupt dehydration could originate a strong decrease of clay volume and a consequently detriment of the mechanical properties of the clay as engineering barrier of the Deep Geological Repository.

The Li^+ radius is the smallest one but it exhibits the highest hydration energy (Table 1s S.I.) and can complete its hydration sphere if the aluminosilicate layer charge decreases (Pavón et al., 2014). This is the reason why higher temperature is required to produce the dehydration as observed in Figure 2.

The effect that the interlayer cation charge on the dehydration process of the swelling high charge mica is examined for Na-n-Mica, Mg-n-Mica and Al-n-Mica samples by considering the electrostatic factor, *q/r* (Table 1s S.I.).

Fig. 2 reveals that the increase of the *q/r* of the interlayer cation produces an increase in the temperature at which the dehydration process commenced for each aluminosilicate layer charge, which is compatible with a higher electrostatic force between layers and cations.

4.2. Rehydration processes.

In contrast to most clay minerals, partial natural re-hydration does not occur readily (Fig. 2, stage 3, Table 1). Samples homoionizied with Li^+ and Na^+ are able to spontaneous rehydrated regardless

the layer charge of the silicate and they reached their initial hydration state with the forced rehydration (Fig 2, stage 4). K-n-Mica is not able to naturally rehydrate regardless the layer charge of the silicate, however, when rehydration is forced, K-2-Mica is able to partial achieved its initial basal space. This result is probably due to the different cationic radii and enthalpy that these cations exhibit. Li^+ and Na^+ possess a smaller ionic radius and longer hydration enthalpy than K^+ that allow them to complete their hydration sphere regardless the layer charge of the silicate, and, thus, to naturally rehydrate the silicate. However, K-n-Micas, with a greater ionic radius, is only able to rehydrate when the layer charge is 2. In K^+-smectites, repeated wetting-drying cycles produce ordering of layer stacking, accompanied by K^+ fixation (Planson et al., 1979) with these effects more evident as the total layer charge of smectite increases (Eberl et al., 1987; Schultz, 1969).

The relationship of *q/r* in rehydration is observed by comparing the results obtained for the samples homoionized with Na^+, Mg^{+2} and Al^{+3}. When the electrostatic *q/r* factor is small, as in Na^+, rehydration is spontaneous regardless the layer charge of the silicate. However, when this factor increases (3.08 and 6.00 for Mg^{+2} and Al^{+3} respectively, Table 1s, S.I.) spontaneous rehydration only occurs in samples with lower layer charge. This result suggests that in high electrostatic field, the interlayer cations have H_2O-adsorption capabilities dependent on their hydration enthalpy and on the electrostatic parameters of the cations.

VH-XRD experiment contributed with a deeper analysis of the rehydration mechanism of these swelling high charge micas (Fig 3). In the following, the effect of silicate layer charge and the physicochemical properties of the interlayer cations (charge and size) are discussed:

4.2.1. Layer charge influence.

In the rehydration process of X-4-Mica, Li^{+}, Na^{+} and Mg^{+2} samples are able to rehydrate from 0W, (ca. 10 A) to 1W (ca. 12 A). The humidity value where this transition occurs was different for each interlayer cation, being between 20 and 30%. The limited 1W swelling capacity of these micas could imply a benefit for CO_2 sequestration as previously observed for montmorillonite. In those samples, CO_2 intercalation was enhanced with hydration up to 1W, and with further hydration it was decreased (Loring et al., 2014) because H_2O displaces CO_2 from the cation solvation shell (Schaef et al., 2015). However, K-4-Mica and Al-4-Mica were not able to rehydrate even for humidity near 100% RH.

Layer charge decreased facilitates H_2O entering in the interlayer and hence, X-3-Mica and X-2-Mica samples were able to rehydrate although different humidity values were needed to produce the transition. These results are consistent with the natural rehydration process observed before in the Temperature experiment (Fig. 2, stage 3 and 4).

However, this result is in contrast with synthetic saponites with a layer charge between 0.4 and 0.7 (Michot et al., 2005) where rehydration is produced at higher values of relative humidity when layer charge decreases. To explain these results, two factors must be considered: 1) when layer charge increases, an increase in the number of interlayer cations are required to balance the charge. If the number of cations in the interlayer is higher, then the attraction to H_2O increases. 2) When layer charge is high, the attractive forces between the layers increases and, consequently, more H_2O molecules are required to initiate swelling.

In synthetic saponites, the attraction force between the interlayer cations prevails over the electrostatic force between the layers. However, the opposite occurred for X-n-Micas where the layer charge is higher and, hence, a higher amount of water molecules is needed to initiate the rehydration.

4.2.2. Influence of the interlayer cationic radii and charge

An increment of the ionic radius produce that higher relative humidity is needed to reach the rehydration, as seen in the Li-,K- and Na-n-samples. This result shows that the H_2O molecules necessary to initiate this process are greater when the ionic radii increases. Additionally, the increase in the electrostatic factor, *q/r*, observed with Na^+ (*q/r*= 1.05), Mg^{+2} (*q/r*= 3.08) and Al^{+3} (*q/r*= 6.00) samples (Fig. 3) provoke that bigger basal spacings are observed once the sample achieved the rehydration, which indicate that the hydration state occurs not only at one monolayer of water, but at two monolayer. As well, the humidity needed to produce this transition decreased with the *q/r* ratio.

These results are in contrast with those found in montmorillonite saturated with magnesium, where at relative humidity near zero, the hydration state occurs at one monolayer of H_2O. Only 20% RH is required to produce the transition to two monolayers of H_2O (Ferrage et al., 2005). For the samples here, these transitions depend on the layer charge of the aluminosilicate. In the case n=4, the sample rehydrates only to one monolayer of H_2O, but when layer charge decreases, higher hydration states are possible to two monolayer of H_2O in the interlayer. When n=3, the transition to 2W occurs at 70% RH, whereas for n=2, 20% RH is required. These results are consistent with the natural rehydration observed for Mg-n-Mica in the temperature experiment, and show that silicate layer charge plays an important role in the rehydration mechanism of these swelling high charge micas. The origin of the layer charge, located in the tetrahedral sheet in our samples, could be the responsible of this behavior, provoking that the interaction forces between the silicate structure and the interlayer cations to be stronger than in other silicates.

5. CONCLUSIONS

For the first time, the dehydration and rehydration mechanism of a swelling high charge mica family has been analyzed as a function of the charge deficit of the aluminosilicate framework and the chemical composition of the interlayer space.

The ability of the X-n-Mica for a reversible dehydration/rehydration process is a consequence of the repulsive forces due to the interactions between the 2:1 layers and the attractive forces between the interlayer cation and the siloxane surface negative charged. Therefore, thorough the tuning of layer charge and the chemical composition of those synthetic micas, it is possible to produce a tailor-made clay for a specific application.

ACKNOWLEDGMENTS

The authors thank the Junta de Andalucía (Spain) and FEDER (Proyecto de Excelencia de la Junta de Andalucía, project P12-FQM-567), the Spanish State Program R+D +I oriented societal challenges and FEDER (Project MAT2015-63929-R) for financial support. Dr. Pavón received support from Andalucía Talent Hub Program, co-funded by the EU in 7FP, Marie Skłodowska-Curie actions (nº 291780) and the Junta de Andalucía. F.J. Osuna received support from the training researcher program associated with the excellence project of Junta de Andalucía (P12-FQM-567).

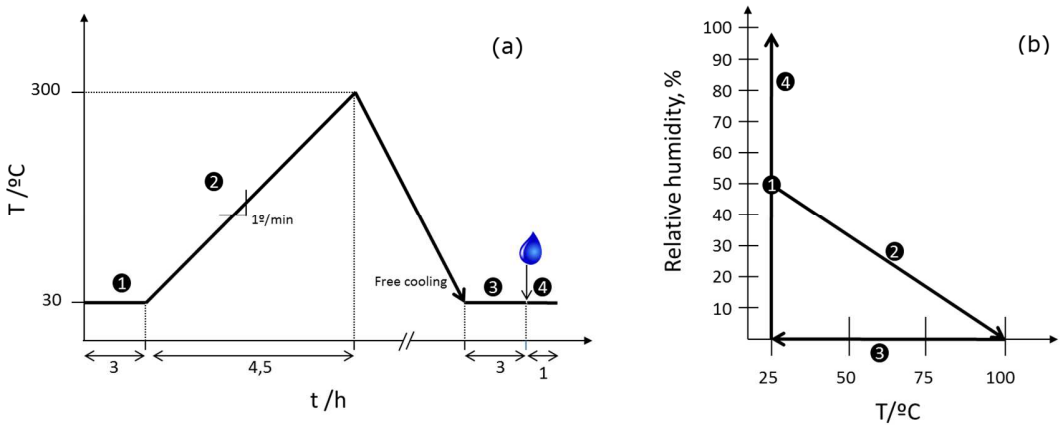

Fig. 1. Schematic representation of the a) Temperature and b) Humidity experiments. Further information on the stages is described in the text

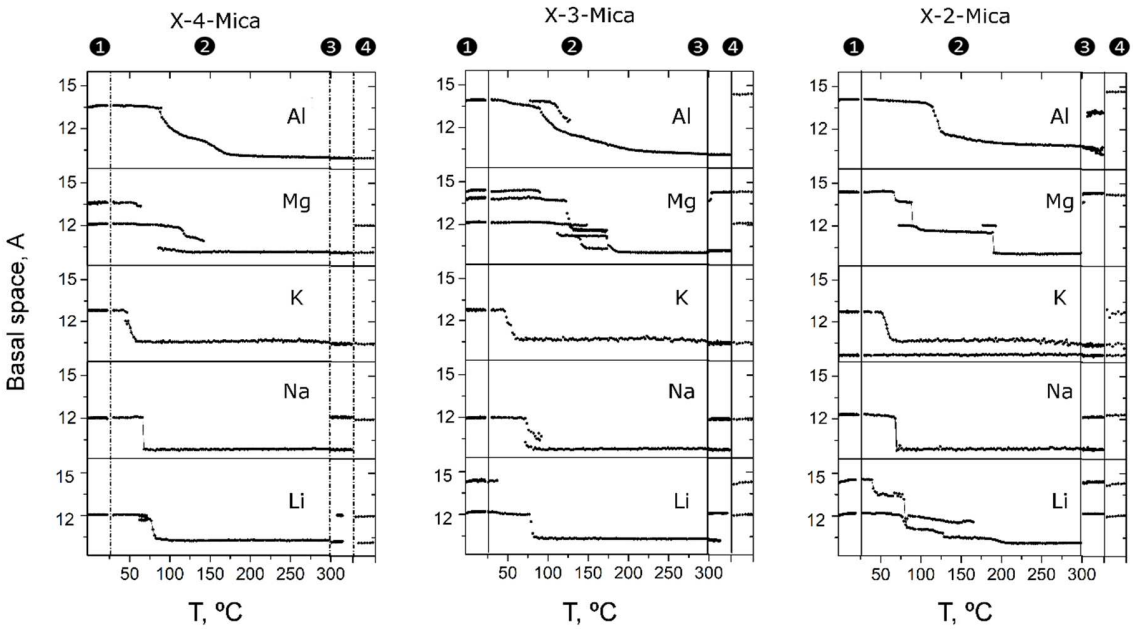

Fig. 2. Evolution of the basal space during the temperature experiment in function of the time (first, third and fourth stages) and temperature (second step) for the set of samples X-n-Mica where X= Li^{+}, Na^{+}, K^{+}, Mg^{+2} and Al^{+3} and n = 2, 3 and 4. First and third stages was 3 h long whereas fourth stage was 1 h. The construction of this figure is explained in Supporting Information.

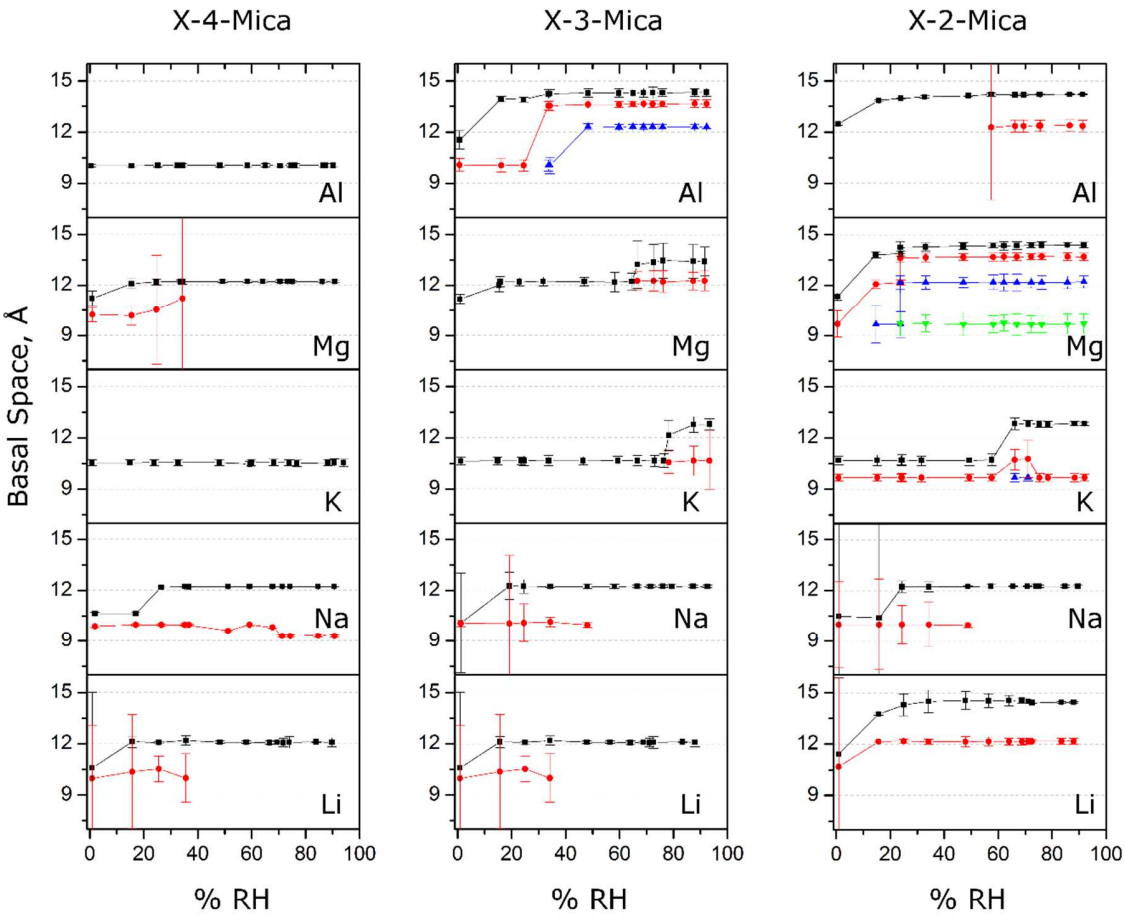

Fig. 3. Basal space in function of relative humidity as obtained during the humidity experiment for the set of samples X-n-Mica where X= Li^{+}, Na^{+}, K^{+}, Mg^{+2} and Al^{+3} and n = 2, 3 and 4. Colours (black, red, blue and green) represent the different 001 reflections observed during the experiments, being black the highest basal spacing and green the lowest one.

Table 1.

Initial Values of Basal Spacing (Å) and after stage 2 (complete dehydration), 3 (free rehydration) and 4 (forced rehydration) in the temperature experiment for the set of samples X-n-Mica where X= Li^{+}, Na^{+}, K^{+}, Mg^{+2} and Al^{+3} and n = 2, 3 and 4.

Interlayer cation	**Initial d_{001} (Å)**	**d_{001} (Å) after heating**	**d_{001} (Å) free rehydrated**	**d_{001} (Å) forced rehydration**
		n=4		
Al	13.5	10.0	10.0	10.0
Mg	13.6	10.2	10.2	12.1
	12.1	-	-	10.2
K	12.8	10.5	10.5	10.5
Na	12.0	9.8	12.0	12.0
	-	-	9.8	-
Li	12.05	10.2	12.0	12.0
	-	-	10.2	10.2
		n=3		
Al	14.0	10.1	10.1	14.4
Mg	14.4	10.2	14.4	14.4
	13.9	-	10.2	12.1
	12.1	-	-	-
K	12.8	10.6	10.6	10.6
Na	12.0	9.8	12.0	12.0
	-	-	9.8	
Li	14.4	-	12.1	12.0
	12.2	10.3	10.3	14.4
		n=2		
Al	14.1	10.8	13.2	14.6
	-	-	10.5	
Mg	14.4	10.0	14.3	14.2
K	12.8	10.7	10.4	12.7
	9.7	9.8	9.7	10.4
	-	-	-	9.7
Na	12.3	9.9	12.1	12.3
		-	9.9	
Li	14.5	10.1	14.5	14.3
	12.1	-	12.1	12.1

Graphical Abstract

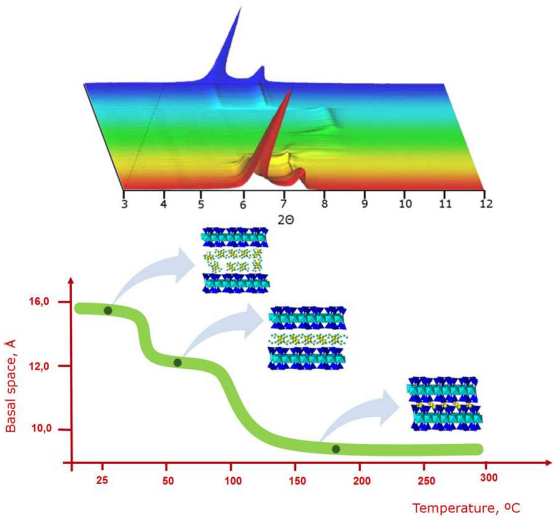

REFERENCES

Alba, M.D., Castro, M.A., Naranjo, M. and Pavón, E. (2006) Hydrothermal reactivity of Na-n-micas (n = 2, 3, 4). Chemistry of Materials 18, 2867-2872.

Alba, M.D., Castro, M.A., Orta, M.M., Pavón, E., Pazos, M.C. and Valencia Rios, J.S. (2011) Formation of organo-highly charged mica. Langmuir 27, 9711-9718.

Amato, I. (2013) Green cement: Concrete solutions. Nature 494, 300-301.

Bergaya, F., Theng, B.G.K. and Lagaly, G. (2006) Handbook of clay sciences. Elsevier, Amsterdam, The Neatherlands.

Bradley, W.F., Grim, R.E. and Clarck, G.L. (1937) A study of the behavior of montmorillonite upon wetting. Zeitschrift Fur Kristallographie 97, 216-222.

Carretero, M.I. (2002) Clay minerals and their beneficial effects upon human health. A review. Applied Clay Science 21, 155-163.

Carretero, M.I. and Pozo, M. (2009) Clay and non-clay minerals in the pharmaceutical industry. Part I. Excipients and medical applications. Applied Clay Science 46, 73-80.

Dazas, B., Lanson, B., Delville, A., Robert, J.L., Komarneni, S., Michot, L.J. and Ferrage, E. (2015) Influence of tetrahedral layer charge on the organization of interlayer water and ions in synthetic Na-saturated smectites. Journal of Physical Chemistry C 119, 4158-4172.

Eberl, D.D., Środoń, J. and Northrop, H.R. (1987) Potassium Fixation in Smectite by Wetting and Drying, Geochemical Processes at Mineral Surfaces. American Chemical Society, pp. 296-326.

Ferrage, E., Lanson, B., Sakharov, B.A. and Drits, V.A. (2005) Investigation of smectite hydration properties by modeling experimental X-ray diffraction patterns: Part I: Montmorillonite hydration properties. American Mineralogist 90, 1358-1374.

Gregorkiewitz, M. and Rausell-Colom, J.A. (1987) Characterization and properties of a new synthetic silicate with highly charged mica-type layers. American Mineralogist 72, 515-527.

Hanczyc, M.M., Fujikawa, S.M. and Szostak, J.W. (2003) Experimental Models of Primitive Cellular Compartments: Encapsulation, Growth, and Division. Science 302, 618-622.

Laird, D.A. (1999) Layer charge infuences on the hydration of expandable 2:1 phyllosilicates. Clays and Clay Minerals 47, 630-636.

Loring, J.S., Ilton, E.S., Chen, J., Thompson, C.J., Martin, P.F., Benezeth, P., Rosso, K.M., Felmy, A.R. and Schaef, H.T. (2014) In Situ Study of CO2 and H2O Partitioning between Na-Montmorillonite and Variably Wet Supercritical Carbon Dioxide. Langmuir 30, 6120-6128.

Macewan, D.M.C. (1948) Clay minerals as catalysts and adsorbents. Nature 162, 195-196.

Malikova, N., Cadènea, A., Dubois, E., Marry, V., Durand-Vidal, S., Turq, P., Breu, J., Longeville, S. and Zanotti, J.M. (2007) Water diffusion in a synthetic hectorite clay studied by quasi-elastic neutron scattering. Journal of Physical Chemistry C 111, 17603-17611.

Malikova, N., Dubois, E., Marry, V., Rotenberg, B. and Turq, P. (2010) Dynamics in clays - Combining neutron scattering and microscopic simulation. Zeitschrift fur Physikalische Chemie 224, 153-181.

Marry, V., Dubois, E., Malikova, N., Durand-Vidal, S., Longeville, S. and Breu, J. (2011) Water dynamics in hectorite clays: Infuence of temperature studied by coupling neutron spin echo and molecular dynamics. Environmental Science and Technology 45, 2850-2855.

Meunier, A., Petit, S., Ehlmann, B.L., Dudoignon, P., Westall, F., Mas, A., El Albani, A. and Ferrage, E. (2012) Magmatic precipitation as a possible origin of Noachian clays on Mars. Nature Geoscience 5, 739-743.

Michot, L.J., Bihannic, I., Pelletier, M., Rinnert, E. and Robert, J.L. (2005) Hydration and swelling of synthetic Na-saponites: Influence of layer charge. American Mineralogist 90, 166-172.
Michot, L.J., Ferrage, E., Jiménez-Ruiz, M., Boehm, M. and Delville, A. (2012) Anisotropic features of water and ion dynamics in synthetic Na- and Ca-smectites with tetrahedral layer charge. A combined quasi-elastic neutron-scattering and molecular dynamics simulations study. Journal of Physical Chemistry C 116, 16619-16633.
Mooney, R.W., Keenan, A.G. and Wood, L.A. (1952a) Adsorption of water vapor by montmorillonite. I. Heat of desorption and application of BET theory. Journal of the American Chemical Society 74, 1367-1371.
Mooney, R.W., Keenan, A.G. and Wood, L.A. (1952b) Adsorption of water vapor by montmorillonite. II. Effect of exchangeable ions and lattice swelling as measured by X-ray diffraction. Journal of the American Chemical Society 74, 1371-1374.
Norrish, K. (1954) The swelling of montmorillonite. Discussions of the Faraday Society 18, 120-134.
Osuna, F.J., Chain, P., Cota, A., Pavón, E. and Alba, M.D. (2015) Impact of hydrothermal treatment of FEBEX and MX80 bentonites in water, HNO3 and Lu(NO3)3 media: Implications for radioactive waste control. Applied Clay Science 118, 48-55.
Park, M., Lee, D.H., Choi, C.L., Kim, S.S., Kim, K.S. and Choi, J. (2002) Pure Na-4-mica: Synthesis and characterization. Chemistry of Materials 14, 2582-2589.
Pavón, E., Castro, M.A., Cota, A., Osuna, F.J., Pazos, M.C. and Alba, M.D. (2014) Interaction of hydrated cations with mica-n (n = 2, 3 and 4) surface. Journal of Physical Chemistry C 118, 2115-2121.
Pavón, E., Castro, M.A., Naranjo, M., Orta, M.M., Pazos, M.C. and Alba, M.D. (2013) Hydration properties of synthetic high-charge micas saturated with different cations: An experimental approach. American Mineralogist 98, 394-400.
Pazos, M.C., Castro, M.A., Cota, A., Osuna, F.J., Pavón, E. and Alba, M.D. (2017) New insights into surface-functionalized swelling high charged micas: Their adsorption performance for non-ionic organic pollutants. Journal of Industrial and Engineering Chemistry 52, 179-186.
Planson, A., Besson, G., Gaultier, J.P., Mamy, J. and Tchoubar, C. (1979) Qualitative and quantitative study of a structural reorganization in montmorillonite after potassium fixation, Developments in Sedimentology, pp. 45-54.
Ravella, R., Komarneni, S. and Martinez, C.E. (2008) Highly charged swelling mica-type clays for selective Cu exchange. Environmental Science and Technology 42, 113-118.
Rinnert, E., Carteret, C., Humbert, B., Fragneto-Cusani, G., Ramsay, J.D.F., Delville, A., Robert, J.L., Bihannic, I., Pelletier, M. and Michot, L.J. (2005) Hydration of a synthetic clay with tetrahedral charges: A multidisciplinary experimental and numerical study. Journal of Physical Chemistry B 109, 23745-23759.
Salles, F., Bildstein, O., Douillard, J.M., Jullien, M., Raynal, J. and Van Damme, H. (2010) On the cation dependence of interlamellar and interparticular water and swelling in smectite clays. Langmuir 26, 5028-5037.
Salles, F., Bildstein, O., Douillard, J.M., Jullien, M. and Van Damme, H. (2007) Determination of the driving force for the hydration of the swelling clays from computation of the hydration energy of the interlayer cations and the clay layer. Journal of Physical Chemistry C 111, 13170-13176.

Salles, F., Devautour-Vinot, S., Bildstein, O., Jullien, M., Maurin, G., Giuntini, J.C., Douillard, J.M. and Damme, H.V. (2008) Ionic mobility and hydration energies in montmorillonite clay. Journal of Physical Chemistry C 112, 14001-14009.
Salles, F., Douillard, J.M., Bildstein, O., Gaudin, C., Prelot, B., Zajac, J. and Van Damme, H. (2013) Driving force for the hydration of the swelling clays: Case of montmorillonites saturated with alkaline-earth cations. Journal of Colloid and Interface Science 395, 269-276.
Schaef, H.T., Loring, J.S., Glezakou, V.A., Miller, Q.R.S., Chen, J., Owen, A.T., Lee, M.S., Ilton, E.S., Felmy, A.R., McGrail, B.P. and Thompson, C.J. (2015) Competitive sorption of CO2 and H2O in 2:1 layer phyllosilicates. Geochim. Cosmochim. Acta 161, 248-257.
Schultz, L.G. (1969) Lithium and potassium absorption, dehydroxylation temperature, and structural water content of aluminous smectites. Clays and Clay Minerals 17, 115-149.
Suter, J.L., Kabalan, L., Khader, M. and Coveney, P.V. (2015) Ab initio molecular dynamics study of the interlayer and micropore structure of aqueous montmorillonite clays. Geochim. Cosmochim. Acta 169, 17-29.
Teich-McGoldrick, S.L., Greathouse, J.A., Jové-Colón, C.F. and Cygan, R.T. (2015) Swelling Properties of Montmorillonite and Beidellite Clay Minerals from Molecular Simulation: Comparison of Temperature, Interlayer Cation, and Charge Location Effects. Journal of Physical Chemistry C 119, 20880-20891.
Vieillard, P., Blanc, P., Fialips, C.I., Gailhanou, H. and Gaboreau, S. (2011) Hydration thermodynamics of the SWy-1 montmorillonite saturated with alkali and alkaline-earth cations: A predictive model. Geochim. Cosmochim. Acta 75, 5664-5685.
Zabat, M. and Van Damme, H. (2000) Evaluation of the energy barrier for dehydration of homoionic (Li, Na, Cs, Mg, Ca, Ba, Al(x)(OH)(y)(z+) and La)-montmorillonite by a differentiation method. Clay Minerals 35, 357-363.